DOI: 10.13009/EUCASS2019-766

8TH EUROPEAN CONFERENCE FOR AERONAUTICS AND AEROSPACE SCIENCES (EUCASS)

DOI: ADD DOINUMBER HERE

Analysis of satellite vibration response using techniques of digital image correlation

Álvaro Souto Janeiro[1†], *Antonio Fernández López*[1], *Marcos Chimeno Manguan*[1],
Pablo García Fogeda Núñez[1] and Pablo Pérez Merino[2]
[1]*Technical University of Madrid (Universidad Politécnica de Madrid-UPM), department of aeronautics*
Plaza del cardenal Cisneros 3, 28040 Madrid (Spain)
[2]*Fundación Jiménez Díaz Institute for health-care research*
Avda. Reyes católicos, 2, 28040 Madrid
antonio.fernandez.lopez@upm.es · marcos.chimeno@upm.es
pablo.garciafogeda@upm.es · pablo.perezm@quironsalud.es
[†]Corresponding author: alvaro.souto.janeiro@alumnos.upm.es

Abstract

A novel methodology to measure the vibration response of a structure using Three-Dimensional Digital Image Correlation techniques (3D-DIC) is presented. 3D-DIC uses the image of a surface pattern, which deforms together with the surface, to measure the deformation of a sample. In the proposed methodology, the speckle is projected on the surface. Therefore, deformation of speckle acquires a crucial importance in the displacement results when analysis is not even and it is not parallel to the camera plane. This proposed technique it is demonstrated on the surface of a satellite and an unmanage aerial vehicle (UAV).

1. Introduction and background

The dynamic response of mechanical components is a critical issue in a large number of industrial fields. In particular, in the field of aeronautics, the response of structures have a key importance because they are sligthtly oversized and they should be designed to work under high vibrations.

The most common technique for characterizing the mechanical response of a structure consists in exciting the structure with a shaker and measuring its dynamics response with a discrete number of accelerometers. As the number of accelerometers is limitted due to the fix and cabling, before placing them in the structure an analysis of the optimal location must be made. It should be noted that accelerometers must be placed in the regions that best characterize the response of the structure. For this purpose, the experience of the staff and structural simulations of the structure is crucial.

Evidently, this technique has two important disadvantages. The first one is that it is not possible to obtain a full area of response from the structure. It is only possible to obtain the response of the structure at discrete points. The other disadvantage is that it is an invasive technique. Accelerometers must be bounded on the structure. This means that it is generally not possible to locate them at the desired positions because other structural elements such as solar panels impede it.

In order to overcome these disadvantages, it is proposed a technique based on digital correlation of images (DIC) as an alternative or complementary method to analyze the mechanical response of structures.

Digital image correlation has been widely employed for measurement deformations in scientific and engineering applications for many years. In 1985 Shih-heng Tung and Chung-huan Sui published the first article of a research on deformations of an object using digital images [18]. The authors obtained a full-field measurement in small regions of the object by comparing images before and after applying a load.

Subsequently, the development of more precise digital cameras, providing advances in the acquisition of images [16], as well as more elaborated algorithms (Newton-Raphson algorithm) possible due to the improvement in data processing, lead to the development and advancement of the DIC techniques.

Three-dimensional Digital image correlation (3D-DIC) is an innovative non-contact optical technique for measuring strain and displacement with high temporal and spatial resolution; it is commonly used in mechanical characterization and has kept booming last years due to its simplicity, robustness and accuracy. 3D-DIC has been employed in a wide variety of applications. Among all of them, for example, Sutton et al. employed the technique to obtain displacement and

DOI: 10.13009/EUCASS2019-766

strain measurement on mouse carotid arteries [15] and Hokka et al used the methodology to analyze the displacement and deformation of the myocardial movement during a cardiopulmonary bypass surgery [7].
In current applications of the DIC technique, the speckle is painted directly on the analysis surface. This has several disadvantages: there are a lot of structures which can not be painted on its surface and, in addition, it takes a lot of time to paint the speckle. Furthermore, once the speckle has been painted, it can not be changed. In order to overcome these disadvantages, in this research is proposed a DIC methodology in which the speckle is projected on the analysis surface.

2. DIC conceptual decription

2.1 Configuration

The configuration employed is presented in Figure 1 where there are two cameras placed pointing to the tested structure, the speckle of points was projected with a projector placed between the two cameras and the tested structure bolted to the shaker. It is necessary to noted that the angle between the two cameras must be small in the order of 30°. If the angle between the two cameras is bigger than 30°, the images taken with the left camera will be too deformed with respect to the images taken with the right camera and it will be very difficult to obtain three-dimensional coordinates. Moreover, the distance between the tested structure and the cameras must be small enough so that the displacements obtained with the cross correlation are at least greater than one pixel.

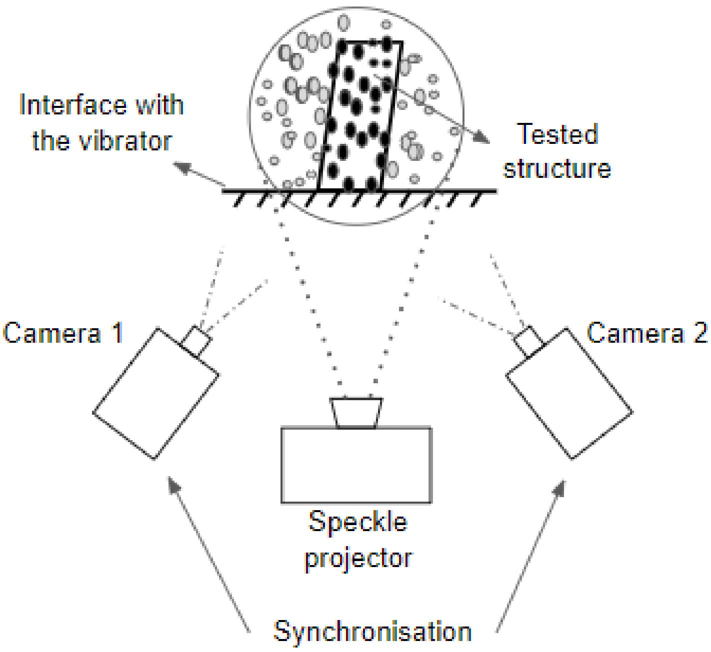

Figure 1: Test configuration.

The proposed methodology is based on two cameras with high acquisition of data. The sampling rate should be considerably higher than the frequency at which the structure is excited to be able to characterize the vibration modes of the structure. The Nyquist criterion states that a sampling frequency of at least twice the excitation frequency is necessary. However, to facilitate accurate shape measurements, a sampling frequency of approximately 10 times the excitation frequency has been chosen, thus a sampling frequency of 1000 Hz has been employed.
Finally, the cameras were synchronized to obtain the three-dimensional coordinates of left and right camera for the application of cross-correlation on the combined images.

2.2 General 3D-DIC procedure

The proposed methodology is shown in Figure 2. The procedure shown in this Figure is a typical one for the 3D-DIC methodology.

DOI: 10.13009/EUCASS2019-766

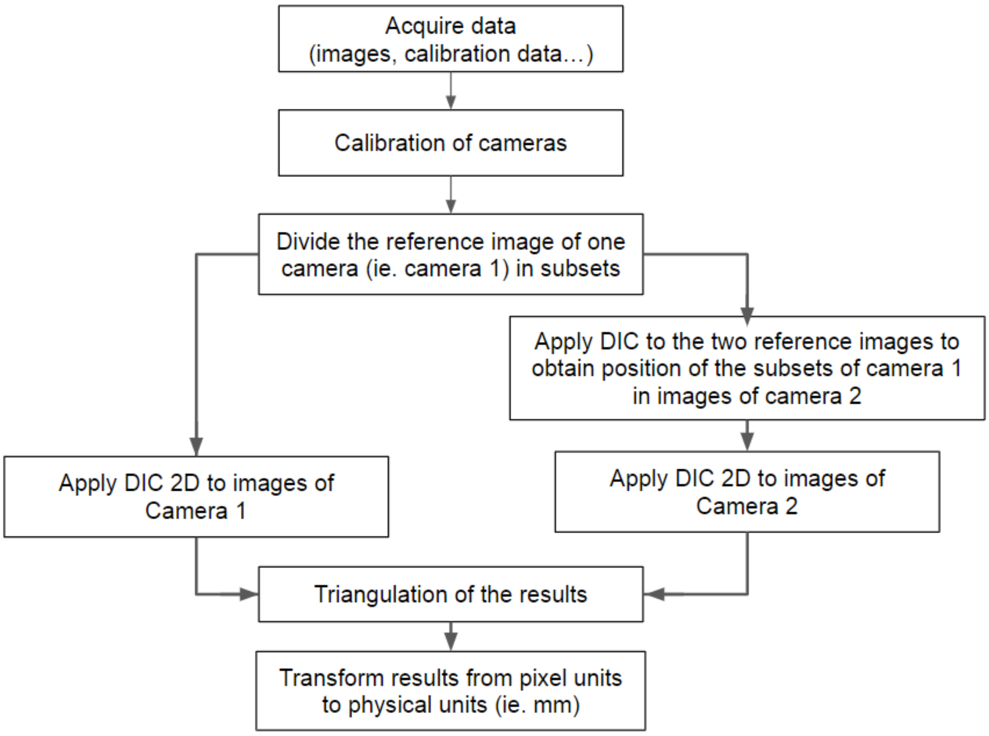

Figure 2: Procedure employed to apply 3D-DIC.

Firstly, reference images were obtained in the unloaded state (reference) to set the origin coordinates of the speckle pattern and the configuration of the subsets to calculate the intrinsic and extrinsic parameters.

After that, intrinsic and extrinsic parameter should be calculated. Several options can be employed for this purpose. The first one consists in solving the equation (3). Another one, quite often employed is to use the Matlab toolbox CalTech Vision. This toolbox was implemented by Jean Yves Bouguet and explained in his doctoral thesis. More information related to this free Matlab toolbox can be found in sources [4], [2] and [3]. Finally, the last option is to employ commercial software as Correlation Solutions software.

The next step is to choose the reference image of one of the cameras. In Figure 2, the reference image of the first camera was chosen. After that, this reference image is divided in smaller image regions, called each one a subset. In Figure 6 is shown an example of this reference image divided in subsets. It is possible to appreciate in this Figure that a subset is a small region of the image of a size of the order of several tens of pixels sideways.

After dividing the reference image of the first camera into subsets, cross correlation should be applied between the reference images of the two cameras. This process is necessary to obtain the position of the subsets that have been defined in the reference image of the first camera in the reference image of the second camera. It is necessary to emphasize that, in principle, the surface to be analyzed will behave like the surface of a rigid body. Therefore, the displacement field obtained by applying cross-correlation between the two images must be consistent with the theory of rigid body. The motion of each subset a random amount of pixels without any relation criteria with the subsets of its surroundings can not be allowed. If the result is a random displacement field in which the displacement of each subset has no relation with the subsets of its surroundings, means that in the distribution of cross correlation coefficients there is no clear maximum and the residues are very high. In that case, the size of the subset should be increased to reduce the amplitude of residues in the distribution of cross correlation coefficients. Another option is to apply cross-correlation in regions where the two reference images most resemble each other, this one also reduces residuesf.

The next step is to apply a cross correlation between the reference image of each camera and the rest of images taken during the test with this camera. This issue will allow to obtain the field of displacements at each instant in which images were taken with respect to the reference image.

Until now, displacements have been obtained and their coordinates are referenced to the image plane. To obtain points and displacement in three-dimensional coordinates the results must be triangulated employing intrinsic and extrinsic parameters of the two cameras.

Finally, the results obtained should be transformed from pixel units to physical units like millimetres.

DOI: 10.13009/EUCASS2019-766

2.3 Extrinsic and intrinsic parameters of the camera

The calibration of the cameras plays a crucial role in the 3D DIC procedure. The parameters obtained in the process of calibration are required for three-dimensional reconstruction of the displacements calculated with each camera.
The technique recommended for the calibration due to its high accuracy and easy implementation, is the planar calibration technique proposed by Zhengyou Zhang in [20]. With this methodology, it is only necessary a set of several images of a plane surface, with a specific pattern printed on its surface, under different orientations. It should be noted that this set of images taken for calibration before the experiment should be taken in different positions covering the largest possible area of the surface of analysis.
The parameters that result from the calibration process can be classified into extrinsic and intrinsic parameters of cameras.

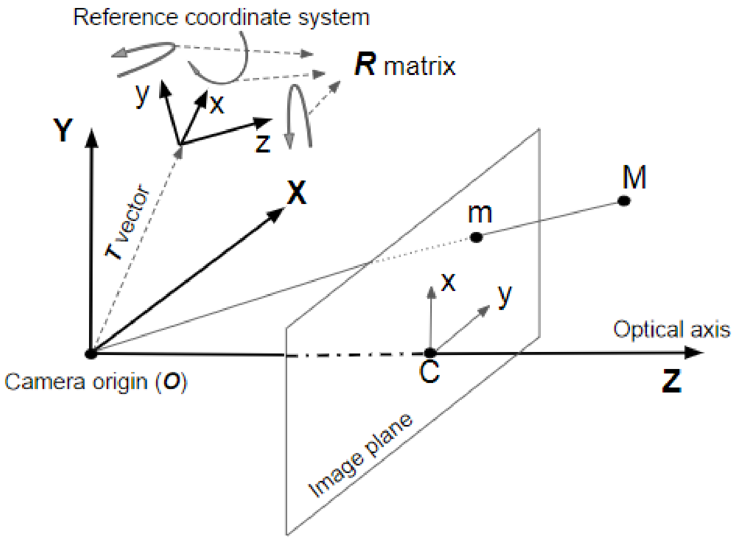

Figure 3: Representative schem of the camera's coordinate system.

The extrinsic parameters relate the position, with a translation vector T, and the orientation of the real world coordinate system with respect to the camera's coordinate system, with a rotation matrix R of 3 by 3 dimension. In Figure 3 the real world coordinate system is named reference coordinate system. Through the combination of the translation vector with the rotation matrix it is obtained the matrix of extrinsic parameters of the camera's system. This matrix is given in the following equation,

$$\left[\begin{array}{c|c} R & T \\ \hline 0 & 1 \end{array}\right] = \left[\begin{array}{ccc|c} r_{1,1} & r_{1,2} & r_{1,3} & t_1 \\ r_{2,1} & r_{2,2} & r_{2,3} & t_2 \\ r_{3,1} & r_{3,2} & r_{3,3} & t_3 \\ 0 & 0 & 0 & 1 \end{array}\right]. \tag{1}$$

Either of these two matrices serve to transform points at the real world coordinate system to the camera's coordinate system. The translation vector represents the position of the real world coordinates system in the camera's coordinates system and columns of the rotation matrix represent the three directions of the axes of the real world coordinate system in the camera's coordinate system.
The intrinsic parameters of a camera define its internal geometry of it and it is related to its optics. Those parameters remain constant as long as the characteristics and relative positions between the camera optics and its CCD system do not change. The matrix of intrinsic parameters is defined in the following expression,

$$B = \begin{bmatrix} f_x & s & C_x \\ 0 & f_y & C_y \\ 0 & 0 & 1 \end{bmatrix}. \tag{2}$$

The parameters C_x and C_y are the coordinates of the point C, shown in Figure 3. This point is the result of intersect the image plane with the optical axis.

DOI: 10.13009/EUCASS2019-766

The other three parameters are related to the geometry of the matrix of sensors of the digital camera. This matrix of sensors are normally placed forming a parallelogram. The coefficients f_x and f_y are related to the size of the sides of this parallelogram. The last coefficient named *skew* and denoted by s represents the inclination of this paralellogram.
Through the combination of the extrinsic parameters and the intrinsic parameters, it is possible to relate the coordinates of a point in the camera plane with the three-dimensional coordinates of this same point. A three-dimensional point is defined by $M = [X, Y, Z, 1]^T$ and its coordinates in the image plane are given by $m = [u, v, 1]^T$. The relation between the point M and its projection is defined by the following equation,

$$\lambda \begin{bmatrix} u \\ v \\ 1 \end{bmatrix} = P \begin{bmatrix} X \\ Y \\ Z \\ 1 \end{bmatrix} = \begin{bmatrix} f_x & s & C_x \\ 0 & f_y & C_y \\ 0 & 0 & 1 \end{bmatrix} \begin{bmatrix} r_{1,1} & r_{1,2} & r_{1,3} & t_1 \\ r_{2,1} & r_{2,2} & r_{2,3} & t_2 \\ r_{3,1} & r_{3,2} & r_{3,3} & t_3 \\ 0 & 0 & 0 & 1 \end{bmatrix} \begin{bmatrix} X \\ Y \\ Z \\ 1 \end{bmatrix}, \tag{3}$$

it should be emphasized that λ is an arbitrary scale factor and P is the projection matrix of the camera.

2.4 Cross correlation

Cross-correlation represents a measure of similarity between two functions, $x(t)$ and $y(t)$. The definition of the cross correlation in time domain responds to the following equation,

$$R_{xy}(\tau) = \int_{-\infty}^{\infty} x(t)y(t+\tau)dt. \tag{4}$$

Cross correlation is, normally, employed to find relevant characteristics in an unknown signal or vector by comparison with another vector or known signal. The second signal usually corresponds to a later time with respect to the known signal. Discreetizing the equation 4 the result is shown in the equation:

$$R_{xy} = \sum_{i,j} (x - \overline{x})(y - \overline{y}), \tag{5}$$

where N represents the number of vector elements of the lagest vector.
There are many variants of the cross correlation coefficient, being one of the best known the normalized cross correlation which is denoted by *NCC*. The principal difference with respect to the single cross correlation is that the minimun and maximun value of the normalized cross correlation is delimited between −1 and 1. The equation of this coefficient is presented in the following mathematic expression,

$$NCC_{xy}(l) = \frac{\sum_{i,j}(x - \overline{x})(y - \overline{y})}{\sqrt{\left[\sum_{i,j}(x - \overline{x})\right]\left[\sum_{i,j}(y - \overline{y})\right]}}. \tag{6}$$

From a practical point of view, Matlab has implemented several cross-correlation functions. In particular, two functions that allow to calculate the cross-correlation between two one-dimensional signals or vectors are *xcorr* and *crosscorr*. The first one calculates the distribution of cross correlation coefficients between the two arrays. The second function obtains the distribution of normalized cross correlation coefficients. Moreover, it should be emphasized that Matlab provides other function to calculate cross correlation coefficients, particularly *normxcorr2*. This function allows to obtain cross coefficients between two two-dimensional signals directly.

3. Experimetal setup

In Figure 4 it is shown the experimental setup for the wing tests. As shown in this Figure, the system employed is constituted by two cameras, a speckle projector and the structure which is screwed to the shaker.
The camera's system employed was VIC 3D HS developed by the company named Correlation Solutions. This camera's system allows to obtain images with a maximun sampling frequency of 900 kHz. The resolution of images depend on the sampling frequency. The higher the value of the sampling frequency, the lower the resolution of the images taken. For a sampling frequency of 1000 Hz, value of the frequency employed to develop all the tests of the wing, the maximum allowed resolution is 1024 by 1024 pixels.

DOI: 10.13009/EUCASS2019-766

The speciment under test is the horizontal tail plain (HTP) of the DIANA Unmanage Aereal Vehicle (UAV). DIANA is a target high speed UAV. It is full made with CFRP AS4/8552 prepreg, and it is composed of two skins with changes in thickness, a longitudinal stringer and two frames in the borders. It is 445mm longh and 265mm wide. All the mechanical joints are made with adhesive.

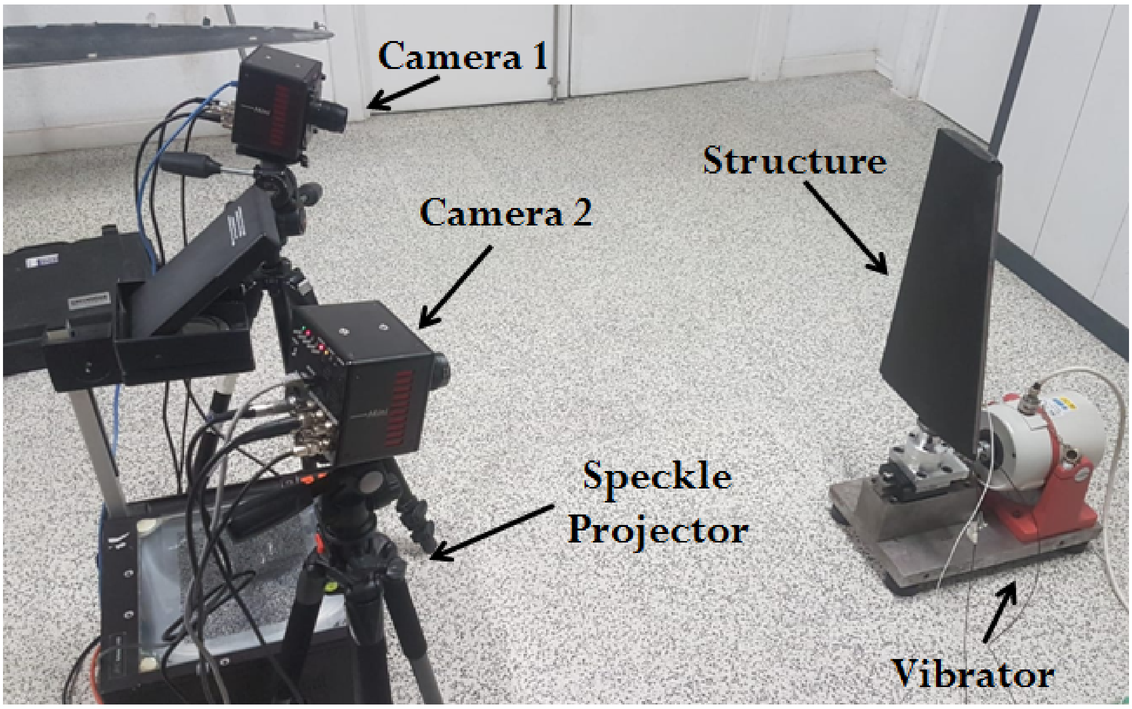

Figure 4: Experimental setup for wing tests.

4. Experimental results of UAV structure

First of all, a frequency sweep from 0 Hz to 100 Hz was performed to obtain the first natural frequencies of the structure. The natural frequencies obtained are shown in the Table 1. After that, the structure was excited at each natural frequency and data was acquired with a 3D-DIC system.

Table 1: First Natural frequencies of the wing in the range of 0 Hz to 100 Hz.

Natural frequency	Type of mode
42.8 Hz	Bending
57.5 Hz	Twisting
83.1 Hz	Twisting
97.5 Hz	Twisting

Once the images have been taken, according to the procedure explained in the section 2.2, it is necessary to choose a subset size and divide the reference image into subsets. It should be noted that as the size of the subset decreases, the probability that the cross correlation provides erroneous displacements increases mainly for two reasons. Firstly, decreasing the subset size increases the magnitude of the residual correlation coefficients, which increases the probability of obtaining wrong displacements.On the other hand, the smaller the size of the subset, the greater the probability that any of the subsets is empty, without any speckle point in its interior. In the case of applying the cross correlation to an empty subset, the displacement obtained will be a random number.
Three different subset sizes were considered: 20x20 pixels, 30x30 pixels and 40x40 pixels. In Figure 5 the distribution of cross correlation coefficients for the three sizes is presented. In this Figure it can be observed that for a subset size of 20 x 20 pixels cross correlation residues reach values comparable to the maximum value of cross correlation coefficients. Therefore, this size is discarded. The other two sizes provide good results, as it can be observed in Figure 5. Thus, the smaller of the two sizes is selected: 30 x 30 pixels subset size.

DOI: 10.13009/EUCASS2019-766

In Figure 6 the subset mesh is presented, represented in blue colour. This mesh was employed to obtain the results shown in Figures 7 to 10.

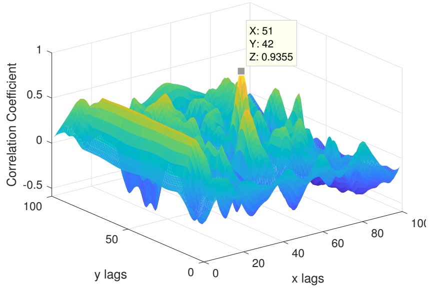

(a) Subset size: 20 x 20 pixel

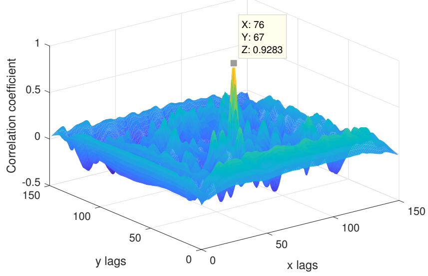

(b) Subset size: 30 x 30 pixel

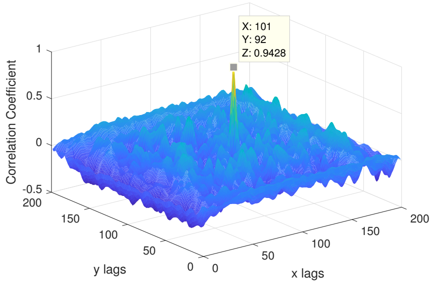

(c) Subset size: 40 x 40 pixel

Figure 5: Distribution of cross correlation coefficients for three different sizes of subset.

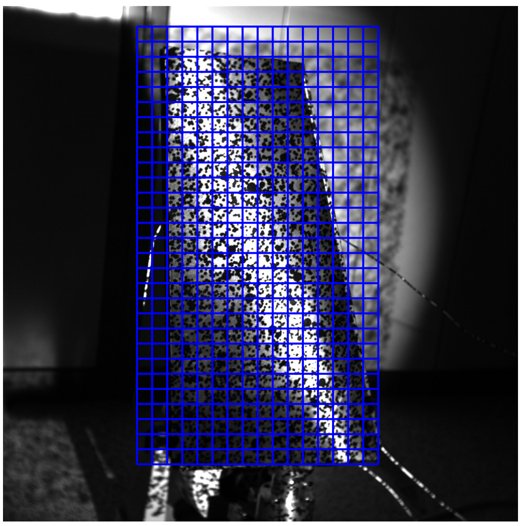

Figure 6: Reference image divided in square subsets of 30 by 30 pixel sideways.

In Figures 7 to 10, the amplitude of displacements of the structure is represented for each one of the four natural frequencies indicated in Table 1. To obtain the amplitude of displacement it was applied the expression,

$$D = \sqrt{d_X^2 + d_Y^2 + d_Z^2}, \tag{7}$$

where d_X, d_Y and d_Z represent the displacement of each component and D respresents the total displacement.

Moreover, it should be noted that in Figures 7 to 10 it is presented the wing deformation at an instant of time while the structure is being excited to one of the natural frequencies. The wing deformation is shown through the views whose orientation is indicated in the Table 2. In those Figures the sign of the displacement was taken into account. Therefore, parts of the wing with positive displacement represent an area of the wing which has deformed in the opposite direction to areas with negative displacement. The parts of the wing with null displacement represent a wing area that has not been deformed.

Remarkably, due to edge effects it was difficult to obtain accurate results in the contour of the wing under vibration; so, these subsets were removed in the presented results.

Table 2: Orientation of each view represented in FIgures 7 to 10.

	Azimuth	**Elevation**
Plan view	0°	0°
Right lateral view	−30°	40°
Left lateral view	30°	40°

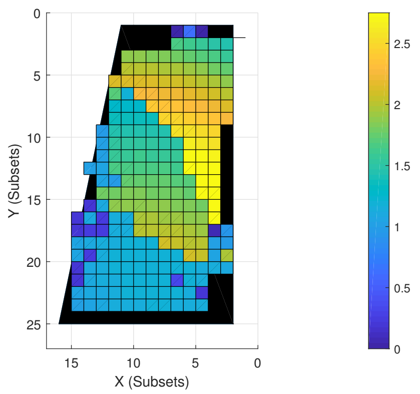

(a) Plan view

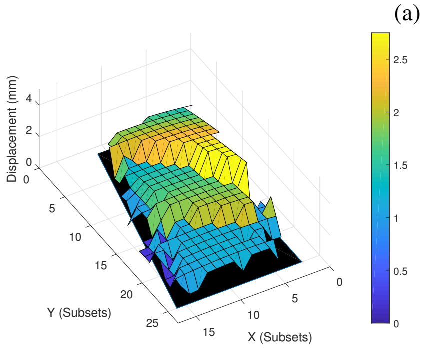

(b) Right lateral view

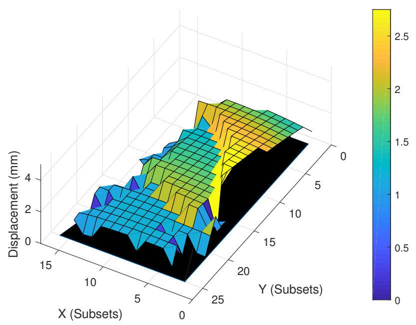

(c) Left lateral view

Figure 7: Static representation of the vibration mode corresponding to an excitation frequency of 41.8 Hz.

DOI: 10.13009/EUCASS2019-766

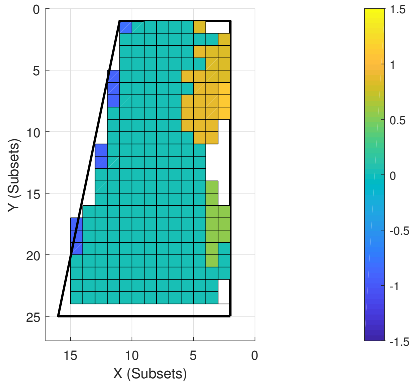

(a) Plan view

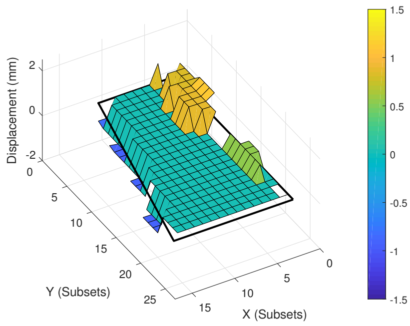

(b) Right lateral view

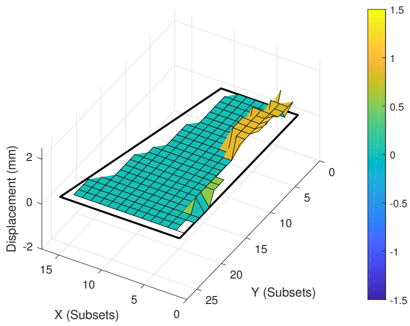

(c) Left lateral view

Figure 8: Static representation of the vibration mode corresponding to an excitation frequency of 57.5 Hz.

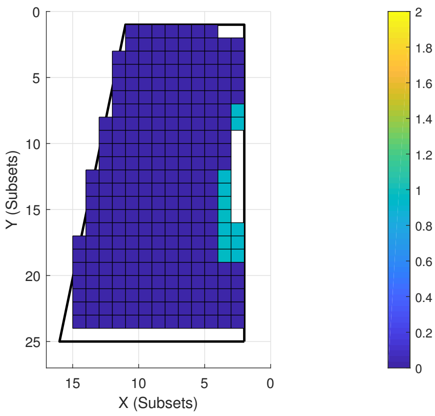

(a) Plan view

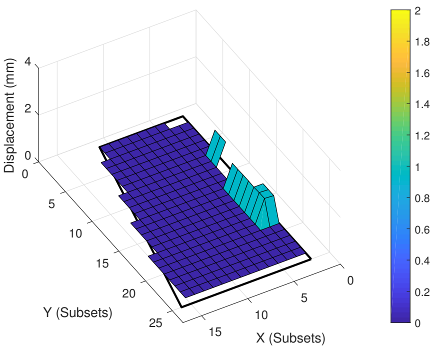

(b) Right lateral view

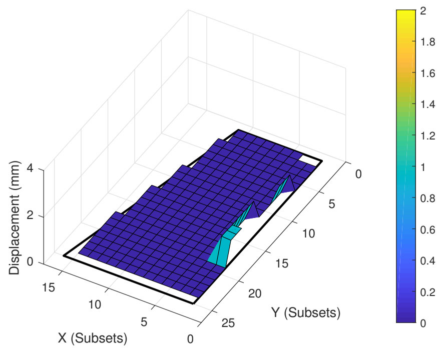

(c) Left lateral view

Figure 9: Static representation of the vibration mode corresponding to an excitation frequency of 83.1 Hz.

DOI: 10.13009/EUCASS2019-766

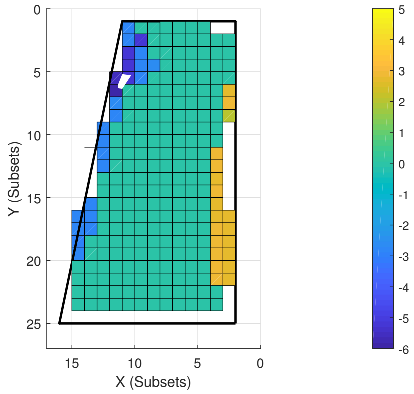

(a) Plan view

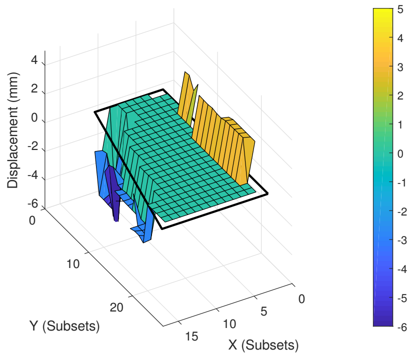

(b) Right lateral view

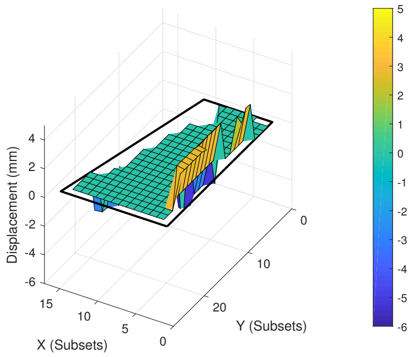

(c) Left lateral view

Figure 10: Static representation of the vibration mode corresponding to an excitation frequency of 97.5 Hz.

5. Experimental results on a satellite

The UPMSAT-2 is a university satellite made by the Institute of Microgravity Ignacio Da Riva of the Polytechnic University of Madrid (IDR/UPM) as a continuation of the UPMSat-1, launched in 1995. The project began in 2009 as a challenge for the institute staff and as a technological demonstrator.

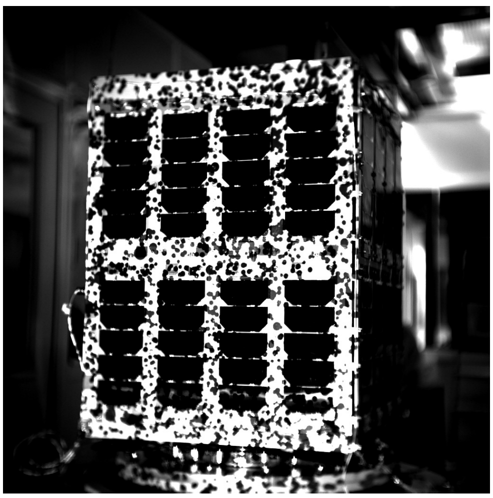

(a) Left camera image

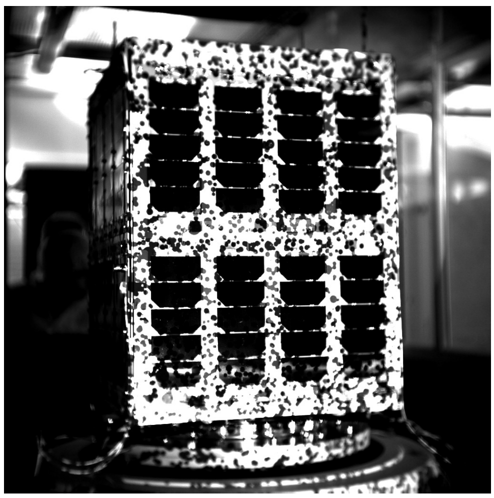

(b) Right camera image

Figure 11: Images of UPMSAT-2 taken with left camera (a) and with right camera (b).

DOI: 10.13009/EUCASS2019-766

The UPMSAT-2 can be defined as a microsatellite with a mass of 50 kg and a parallelepiped shape whose base is 0.5 m by 0.5 m in dimension and its height is 0.6 m. It allows to carry payloads with a maximum volume of 0.4 m by 0.4 m by 0.25 m, a maximum power consumption of 15 W and a maximum mass of 15 kg. More information related to UPMSAT-2 can be found in sources [11] and [9].
Currently, the experimental results of the test performed on the UPMSat-2 are under analysis.

6. Conclusions

In this article, it is proposed a methodology based in digital image correlation to measure dynamics response of mechanical structures. The principal advantages of this technique is that it is a non-invasive methodology and it provides measurements along a surface. This makes it an ideal technique to measure the response of satellites, whose faces are usually covered by solar cells or other devices that make it difficult the measure of the dynamics response.
The principal difference of the proposed DIC methodology, with respect to existing DIC techniques employed to study structural and material behavior, is that instead of painting the speckle on the surface of the structure in this case the speckle is projected on the surface. This aspect makes the shape of the points of speckle become very important in the application of cross correlation. Therefore, residues cross correlation coefficients acquire a crucial role.
In order to validate or demostrate the deployment of the proposed methodology to measure the response of mechanical structures, the technique was applied to mechanical tests performed on a piece of wing made of composite material. The high level of accuracy of the measurement technique and the capability to identify the dynamic mode (shape and intensity) proofs the high potential and capabilities of 3D-DIC with projected speckle. In addition, the technique has been employed to measure the dynamics response of the UPMSAT-2 where the limitation introduced by solar panels and other fuctional elements do not allow to use traditional measurement techniques, such accelerometers or painted DIC. The projected speckle pattern presents significant advances over the speckle pattern painting, however it requires dedicated image processing tools to evaluate the out-of-plane displacements and the residual cross correlation coefficients. The high level of accuracy of the proposed methodology to identify the dynamic mode in terms of shape and intensity will allow in-depth non invasive material characterization.

7. Acknowledgments

This reseach is supported by the Institute of Microgravity Ignacio Da Riva of the Polytechnic University of Madrid (IDR / UPM) and the Master's degree in Space Systems (MUSE). This study was also supported by Spanish Government grant: DTS18/00107. The authors indicate the following financial disclosure: PCT/ES2018/070757 Dispositivo y procedimiento de obtención de medidas mecánicas, geométricas y dinámicas de superficies ópticas (Pablo Pérez Merino y Antonio Fernández López).

References

[1] Sandro Barone, Paolo Neri, Alessandro Paoli, and Armando Razionale. Digital image correlation based on projected pattern for high frequency vibration measurements. *Procedia Manufacturing*, 11:1592–1599, 2017.

[2] Jean-Yves Bouguet. Visual methods for three-dimensional modeling. Available: `http://www.vision.caltech.edu/bouguetj/calib_doc/`, 2015 (accessed May 13, 2019).

[3] Jean-Yves Bouguet. Camera calibration toolbox for matlab. Available: `http://www.vision.caltech.edu/bouguetj/`, 2015 (accessed May 23, 2019).

[4] Jean-Yves Bouguet et al. *Visual methods for three-dimensional modeling*. Citeseer, 1999.

[5] Shaoyan Gai, Feipeng Da, and Xianqiang Dai. Novel 3d measurement system based on speckle and fringe pattern projection. *Optics express*, 24(16):17686–17697, 2016.

[6] Takeshi Hashimoto, Takayuki Suzuki, Hidemichi Aoshima, and András Rövid. Multi-camera-based high precision measurement approach for surface acquisition. *Acta Polytechnica Hungarica*, 10(8):139–152, 2013.

[7] Mikko Hokka, Nikolas Mirow, Horst Nagel, Marc Irqsusi, Sebastian Vogt, and Veli-Tapani Kuokkala. In-vivo deformation measurements of the human heart by 3d digital image correlation. *Journal of biomechanics*, 48(10):2217–2220, 2015.

DOI: 10.13009/EUCASS2019-766

[8] Mamoru Miura, Shuji Sakai, Jumpei Ishii, Koichi Ito, and Takafumi Aoki. An easy-to-use and accurate 3d shape measurement system using two snapshots. *Proc. IWAIT 2013*, pages 1103–1106, 2013.

[9] Institute of Microgravity Ignacio Da Riva (IDR/UPM). Upmsat-2. Available: `http://www.idr.upm.es/index.php/es/el-proyecto-upm-sat-2`, (accessed May 30, 2019).

[10] Rubén Salazar Polo. *Validación experimental de la distribución de deformaciones en una unión adhesiva mediante técnicas de correlación de imágenes*. TFM, Universidad Politécnica de Madrid, June 2014.

[11] Ali Ravanbakhsh and Sebastian Nicolas Franchini. Preliminary structural sizing of a modular microsatellite based on system engineering considerations. 2010.

[12] Hubert W Schreier. Investigation of two and three-dimensional image correlation techniques with applications in experimental mechanics. 1969.

[13] Xinxing Shao, Xiangjun Dai, Zhenning Chen, and Xiaoyuan He. Real-time 3d digital image correlation method and its application in human pulse monitoring. *Applied optics*, 55(4):696–704, 2016.

[14] José Ramón Conde Suárez. *Estudio de las deformaciones fuera del plano en superficies mediante técnicas de correlación de imágenes*. TFM, Universidad Politécnica de Madrid, September 2015.

[15] MA Sutton, X Ke, SM Lessner, M Goldbach, M Yost, F Zhao, and HW Schreier. Strain field measurements on mouse carotid arteries using microscopic three-dimensional digital image correlation. *Journal of Biomedical Materials Research Part A: An Official Journal of The Society for Biomaterials, The Japanese Society for Biomaterials, and The Australian Society for Biomaterials and the Korean Society for Biomaterials*, 84(1):178–190, 2008.

[16] Michael A Sutton, Stephen R McNeill, Jeffrey D Helm, and Yuh J Chao. Advances in two-dimensional and three-dimensional computer vision. In *Photomechanics*, pages 323–372. Springer, 2000.

[17] Michael A Sutton, Jean Jose Orteu, and Hubert Schreier. *Image correlation for shape, motion and deformation measurements: basic concepts, theory and applications*. Springer Science & Business Media, 2009.

[18] Shih-Heng Tung and Chung-Huan Sui. Application of digital-image-correlation techniques in analysing cracked cylindrical pipes. *Sadhana*, 35(5):557–567, 2010.

[19] Jae-Chern Yoo and Tae Hee Han. Fast normalized cross-correlation. *Circuits, systems and signal processing*, 28(6):819, 2009.

[20] Zhengyou Zhang. A flexible new technique for camera calibration. *IEEE Transactions on pattern analysis and machine intelligence*, 22, 2000.